Amino Acids (2013) 44:373–381
DOI 10.1007/s00726-012-1340-9

ORIGINAL ARTICLE

Transport of L-proline by the proton-coupled amino acid transporter PAT2 in differentiated 3T3-L1 cells

Katja Zebisch · Matthias Brandsch

Received: 21 December 2011 / Accepted: 4 June 2012 / Published online: 19 June 2012

Abstract Mechanism and substrate specificity of the proton-coupled amino acid transporter 2 (PAT2, SLC36A2) have been studied so far only in heterologous expression systems such as HeLa cells and *Xenopus laevis* oocytes. In this study, we describe the identification of the first cell line that expresses PAT2. We cultured 3T3-L1 cells for up to 2 weeks and differentiated the cells into adipocytes in supplemented media containing 2 μM rosiglitazone. During the 14 day differentiation period the uptake of the prototype PAT2 substrate L-[^{3}H]proline increased ~5-fold. The macro- and microscopically apparent differentiation of 3T3-L1 cells coincided with their H^+ gradient-stimulated uptake of L-[^{3}H]proline. Uptake was rapid, independent of a Na^+ gradient but stimulated by an inwardly directed H^+ gradient with maximal uptake occurring at pH 6.0. L-Proline uptake was found to be mediated by a transport system with a Michaelis constant (K_t) of 130 ± 10 μM and a maximal transport velocity of 4.9 ± 0.2 nmol × 5 min^{-1} mg of protein^{-1}. Glycine, L-alanine, and L-tryptophan strongly inhibited L-proline uptake indicating that these amino acids also interact with the transport system. It is concluded that 3T3-L1 adipocytes express the H^+-amino acid cotransport system PAT2.

Keywords 3T3-L1 cells · SLC36A2 · Membrane transport · PAT2 · Adipocyte

K. Zebisch · M. Brandsch (✉)
Biozentrum of the Martin-Luther-University Halle-Wittenberg, Weinbergweg 22, 06120 Halle, Germany
e-mail: matthias.brandsch@biozentrum.uni-halle.de

Introduction

The proton-coupled amino acid transporter 2 (PAT2) is one of four members of the solute carrier (SLC) family 36 (Boll et al. 2004; Hediger 2004). Originally, the first member of this family was identified as the lysosomal amino acid transporter (SLC36A1, LYAAT1) in rat brain (Sagné et al. 2001). Subsequently, mouse and human homologs were cloned from mouse intestine (Boll et al. 2002) and from Caco-2 cells (Chen et al. 2003a) and named PAT1. The system is very likely identical to the H^+-amino acid cotransporter that had been functionally described in Caco-2 cells (Ranaldi et al. 1994; Thwaites et al. 1993, 1995). Simultaneously to PAT1, the cloning of the H^+-coupled amino acid transporter PAT2 (SLC36A2) from mouse was published (Boll et al. 2002). PAT3, cloned in 2003 (Boll et al. 2003b), still represents an orphan transporter. Regarding PAT4, Pillai and Meredith (2011) could show very recently that this system, when expressed in *Xenopus laevis* oocytes, is an amino acid transporter that in contrast to PAT1 and PAT2 is not proton-coupled.

The function of PAT1 from mouse and human and that of PAT2 from mouse and rat has been studied in great detail in recent years using mainly glycine and L-proline as substrates (Boll et al. 2002, 2003a; Chen et al. 2003a, b; Foltz et al. 2004a, b; Kennedy et al. 2005; Metzner et al. 2004, for reviews see Thwaites and Anderson 2007, 2011). The transport of substrates by these systems across cell membranes occurs strictly in form of an H^+-substrate symport. Prototype substrates for PAT1 and PAT2 are small neutral amino acids (e.g. L-proline, glycine, L-alanine) and derivatives. Compared to the isoform transporter PAT1, PAT2 is classified as the "high affinity, low capacity" transporter (Boll et al. 2002). Interestingly, 5-hydroxy-L-tryptophan and certain derivatives represent

high-affinity, non-transported inhibitors for both hPAT1 (Metzner et al. 2005) and rPAT2 (Edwards et al. 2011). Foltz and co-workers using *X. laevis* oocytes have shown that both PAT1 and PAT2 mediate electroneutral H^+-symport of short-chain fatty acids (Foltz et al. 2004a).

hPAT1, which is expressed at the apical membrane of enterocytes, gained much interest in recent years because the carrier transports pharmaceutically relevant compounds such as D-cycloserine, L-azetidine-2-carboxylic acid, 3-amino-1-propanesulfonic acid, β-guanidinopropionic acid and vigabatrin. Hence, the system is looked on as a possible vehicle for drug delivery in general and for purposes of increasing the bioavailability of drugs (Larsen et al. 2009; Metzner et al. 2004; Thwaites and Anderson 2011). PAT2 research, on the other hand, is currently drawing much attention because the gene encoding PAT2 was identified as the major gene responsible for iminoglycinuria and hyperglycinuria (Bröer et al. 2008). Moreover, a delayed expression and maturation of mPAT2 and other solute carriers give rise to the so called developmental iminoglycinuria, a transient version of iminoglycinuria during renal ontogeny (Vanslambrouck et al. 2010).

The well-established and widely used cultured cell line Caco-2 is available for studies with PAT1 (Chen et al. 2003a; Larsen et al. 2009; Metzner et al. 2004, 2005; Thwaites et al. 1993) whereas no equivalent cell line is available for PAT2. All functional studies on PAT2 had to be carried out using heterologous expression systems, *i.e. X. laevis* oocytes (Boll et al. 2002; Bröer et al. 2008; Chen et al. 2003b; Edwards et al. 2011; Foltz et al. 2004b; Kennedy et al. 2005) and transfected mammalian cells (Chen et al. 2003b). Such a cell line would offer an ideal experimental model for studies on pH dependent amino acid transport and in particular for studies on regulatory aspects such as transporter protein trafficking. In the last years we and other groups investigated many cell lines originating from PAT2-mRNA positive tissues such as kidney, lung, heart, muscle, testis, spleen, adrenal gland, thymus, and nerve tissue (Bermingham et al. 2002; Bermingham and Pennington 2004; Boll et al. 2002; Bröer et al. 2008; Klein et al. 2010; Rubio-Aliaga et al. 2004; Sundberg et al. 2008; Vanslambrouck et al. 2010) without success. Surprisingly, we did not find PAT2 function in any of the renal cell lines tested such as LLC-PK1, Cos-7, HEK-293, OK and SKPT. It seems that—at least under the culture conditions chosen—none of these lines are good models. There was, however, evidence for a strong expression of PAT2 in a more "unlikely", non-epithelial tissue, *i.e.* adipose tissue (Bermingham and Pennington 2004; Sundberg et al. 2008). We confirmed this result in own extensive investigations on SLC36A2 expression in rat tissues using RT-PCR. Next, we examined PAT2 in 3T3-L1 cells. The cell line 3T3-L1 is widely used in studies on adipogenesis and fat tissue function (Green and Kehinde 1974). When we differentiated 3T3-L1 cells for up to 14 days using rosiglitazone-containing medium (Zebisch et al. 2012), we observed a prominent and increasing H^+-stimulated L-proline uptake by PAT2.

This study represents the first identification of a cell line that expresses the amino acid transporter PAT2 and the first characterization of its function in a non-transfected cell.

Materials and methods

Materials

The mouse fibroblast cell line 3T3-L1 (Lot 58432113) was obtained from ATCC (LGC Standards GmbH, Wesel, Germany). Dulbecco's modified Eagle medium (DMEM, high glucose) was purchased from Invitrogen (Karlsruhe, Germany). Fetal bovine serum (FBS), newborn calf serum (NCS), and 100x penicillin/streptomycin (P/S) were from Biochrom (Berlin, Germany). 3-Isobutyl-1-methylxanthine (IBMX), dexamethasone, human insulin, amino acids and derivatives and other chemicals were purchased from Sigma–Aldrich (Taufkirchen, Germany). Rosiglitazone was obtained from Cayman Chemical (Biomol, Hamburg, Germany). Cell culture flasks, 35 mm disposable Petri dishes ("cell+") were purchased from Sarstedt (Nümbrecht, Germany). Trypsin EDTA (10x) was obtained from PAA (Cölbe, Germany). Primers were synthesized and purchased from Biomers (Ulm, Germany).

Culture and differentiation of 3T3-L1 cells

Culture and differentiation of 3T3-L1 cells was carried out as described recently with slight modifications (Zebisch et al. 2012). In brief, 3T3-L1 preadipocytes (passages 5–10 after purchase) were cultured in basal medium I consisting of DMEM containing 10 % NCS, 100 units ml^{-1} penicillin and 100 µg ml^{-1} streptomycin (1x P/S). Cells were maintained in 75 cm^2 culture flasks at 37 °C in a humidified atmosphere with 5 % CO_2. At 80 % confluence, cells were released by trypsinization (1x trypsin EDTA in phosphate buffered saline (PBS)) and subcultured. For transport and RT–PCR studies, cells were seeded in 35 mm dishes at a density of 6×10^5 cells/dish. The day after seeding cells reached confluence and the medium was replaced. For differentiated 3T3-L1 cells the medium was changed 48 h after reaching confluence (day 3) to DMEM containing 10 % FBS, 1x P/S, 0.5 mM IBMX, 0.25 µM dexamethasone, 1 µg/ml insulin and 2 µM rosiglitazone (differentiation medium I). After 72 h (day 6) cells were incubated in DMEM containing 10 % FBS, 1x P/S, and 1 µg/ml insulin (differentiation medium II) for 48 h (day 8) following incubation in DMEM containing

10 % FBS, and 1x P/S (basal medium II). This medium was replaced on days 9, 11, and 13. For undifferentiated 3T3-L1 cells the medium was changed on day 3 to basal medium II and was then replaced on days 6, 8, 9, 11 and 13 (Zebisch et al. 2012).

L-[^{3}H]Proline uptake measurements

Uptake of L-[^{3}H]proline in differentiated and undifferentiated 3T3-L1 cells was measured using uptake buffer containing either 25 mM MES/Tris (pH 6.0) or 25 mM HEPES/Tris (pH 7.4), 140 mM NaCl or 140 mM choline chloride, 5.4 mM KCl, 1.8 mM $CaCl_2$, 0.8 mM $MgSO_4$, 5 mM glucose and 15 nM L-[^{3}H]proline (50 Ci mmol^{-1} specific activity; Perkin Elmer, Rodgau, Germany). For Cl^- -free buffers, the chloride salts (NaCl, KCl and $CaCl_2$) were replaced by the respective gluconate salts. For Na^+ and Cl^-- free buffers NaCl was replaced by 280 mM D-mannitol and KCl and $CaCl_2$ by their respective gluconate salts. For measuring the pH dependence, three uptake buffers were prepared containing either 50 mM HEPES, 50 mM Tris or 50 mM MES and mixed accordingly.

Prior to the uptake experiment, the cells were washed twice with the respective buffer without substrates. Cells were then incubated with 1 ml of the respective uptake buffer containing L-[^{3}H]proline in the absence or presence of unlabeled compounds at room temperature (22–24 °C) for the required incubation time. After the desired incubation periods, the cells were washed quickly four times with ice-cold buffer and lysed by adding 1 ml of lysis buffer (0.2 M NaOH/1 % SDS). After transferring the radioactive cell suspension to a vial, each culture dish was washed with 0.5 ml lysis buffer that was then also added to the respective vial. To each sample 2.8 ml of liquid scintillation cocktail (Rotiszint® ecoplus, Roth, Karlsruhe, Germany) were added and the sample was mixed for at least 10 s on a Vortex-Genie 2 (Scientific Industries, Bohemia, NY, USA). The vials were measured for 5 min by liquid scintillation spectrometry (Tri-Carb 2100TR, Packard Instrument Company, Meridem, CT, USA).

Protein concentration was determined using the Pierce 660 nm protein assay with bovine serum albumin as standard (Fisher Scientific, Schwerte, Germany). For that purpose cells from each uptake experiment were washed twice with buffer and stored at −20 °C. Cells were lysed using ProteoJET™ Mammalian Cell Lysis Reagent (Fermentas, St. Leon-Rot, Germany) containing protease inhibitor (Roche Applied Science, Penzberg, Germany).

RNA isolation and RT-PCR

3T3-L1 cells were cultured in 35 mm dishes as described above. Dishes were washed twice with PBS and the cells were scraped off and stored in 200 µl PBS at −80 °C until RNA isolation. Total RNA was isolated using the High Pure RNA Isolation Kit (Roche Applied Science, Penzberg, Germany). RNA-integrity (18S and 28S ribosomal RNAs bands) was examined by agarose gel electrophoresis using 2 % agarose (Agarose GTQ, Roth, Karlsruhe, Germany) in TAE buffer using the RiboRuler™ High Range RNA Ladder (Fermentas, St. Leon-Rot, Germany). As positive control fat tissue from a 1.5-year-old, 24 h fasting male Wistar rat (Charles River, Sulzfeld, Germany) was used. Total RNA was isolated using the RNeasy Lipid Tissue Kit and RNase-Free DNase Set (Qiagen, Hilden, Germany). The tissue was disrupted with a pestle (no. 03-392-100, Fisherbrand, Schwerte, Germany) and homogenized using QIAshredder (Qiagen, Hilden, Germany). The concentration of RNA was determined by measuring the absorbance at 260 nm in a spectrophotometer (Ultrospec 3300 pro, GE Healthcare, Chalfont St. Giles, UK). The isolated RNA was stored at −80 °C.

RT-PCR was carried out using the OneStep RT-PCR Kit (Qiagen, Hilden, Germany), 0.5 µg of isolated RNA and mouse and rat specific primers for GAPDH (5′- GTGAAG GTCGGTGTGAACGGATTTGG-3′ and 5′-CATCATACT TGGCAGGTTTCTCCAGG-3′) or PAT2 (5′-CAGGTAG TAGAAGCTGTTAACAGCAC-3′and 5′-CAGCCAGCAG TTGGGCAGGTTAAG-3′) at a final concentration of 0.6 µM each. The reverse transcription reaction was allowed to proceed for 30 min at 50 °C. After the initial heating step (95 °C, 15 min) fragments were amplified in 35 PCR cycles (94 °C, 45 s; 62 °C, 45 s; 72 °C, 1 min) and finally extended (72 °C, 10 min) in a thermal cycler (C1000™, BioRad, Munich, Germany). For analysis, 1.5 µl of each GAPDH PCR reaction product and 5.0 µl of each PAT2 PCR reaction product were separated on a 2 % agarose gel (SeaKem® LE Agarose, Lonza by Biozym, Oldendorf, Germany) in TBE-buffer and stained using SYBR® Safe DNA Gel Stain (Invitrogen, Karlsruhe, Germany). For sizing of the DNA fragments GeneRuler™ 100 bp Plus DNA Ladder (Fermentas, St. Leon-Rot, Germany) was used. The expected sizes of the products were 760 bp for GAPDH and 492 bp for PAT2, respectively. Primers were designed across exon–exon boundaries to exclude amplification of genomic DNA. Their specificity was checked using the standard nucleotide BLAST provided by NCBI (http://blast.ncbi.nlm.nih.gov/Blast.cgi).

Data analysis

Experiments were done in duplicates or triplicates and each experiment was repeated two to three times. The data given represent mean ± SE. Nonlinear regression analysis and calculation of inhibition constants (K_i) from IC_{50} values were done as described (Metzner et al. 2004, 2005, 2006).

Statistical analysis was done by the non-parametric two-tailed *U* test and a *P* value of less than 0.05 was considered statistically significant.

Results and discussion

Functional characteristics of L-proline uptake in differentiated 3T3-L1 adipocytes

To determine whether 3T3-L1 cells express the amino acid transporter PAT2, we studied the uptake of the prototype PAT2 substrate L-proline into these cells. By using different media we kept part of the cells in their preadipocyte state and subjected the other part to differentiation to adipocytes. In the course of differentiation, intracellular lipid droplets appeared macroscopically at around day 7 that increased in both number and size over the next days. Full differentiation of the cells was reached not later than day 14 when nearly all of the cells contained lipid droplets of different sizes. In regular culture medium used for undifferentiated preadipocytes, only very few single cells showed small visible lipid droplets that did not change their size over 18 days (Zebisch et al. 2012).

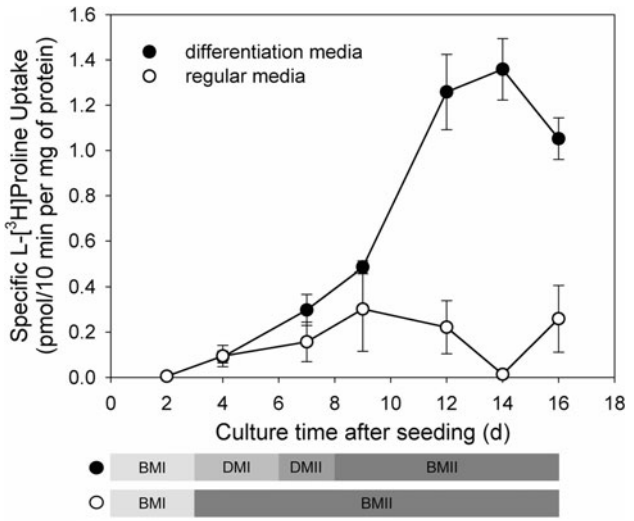

Fig. 1 Influence of growth state on specific L-[^{3}H]proline uptake in 3T3-L1 preadipocytes (*open circle*) and 3T3-L1 cells differentiating to adipocytes (*filled circle*). Cells were seeded in 35 mm dishes at a density of 6×10^5 cells/dish using basal medium I (BMI). For differentiated 3T3-L1 cells the medium was changed 48 h after reaching confluence (day 3) to differentiation medium I (DMI). After 72 h (day 6) cells were incubated in differentiation medium II (DMII) for 48 h (day 8) following incubation in basal medium II (BMII). For undifferentiated 3T3-L1 cells the medium was changed on day 3 to basal medium II. Uptake of L-[^{3}H]proline (15 nM; 10 min; pH 6.0; $-Na^+$) was measured in the presence and absence of 30 mM unlabeled proline. Uptake in the presence of unlabeled proline was subtracted to calculate specific L-[^{3}H]proline uptake. Values are mean ± SE, $n = 4$–6 for each point

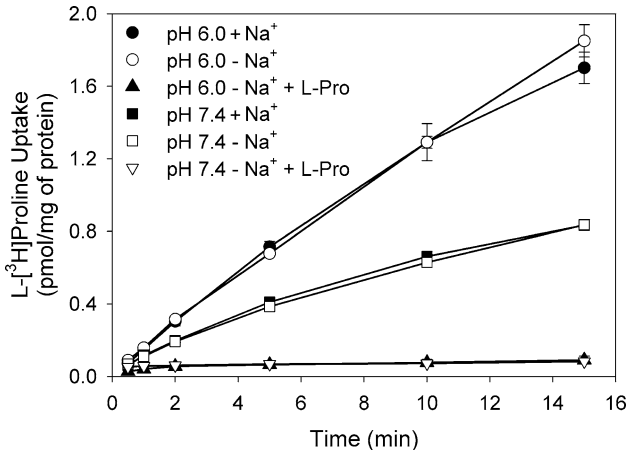

Fig. 2 Time-dependent uptake of L-[^{3}H]proline at pH 6.0 and 7.4 in differentiated 3T3-L1 adipocytes cultured for 14 days. Uptake of L-[^{3}H]proline (15 nM) was measured in the presence or absence of sodium and, in the absence of sodium also in presence of excess amounts of unlabeled L-proline (30 mM). The measured L-[^{3}H]proline uptake (pH 6.0, without sodium, 10 min) was about 77,000 dpm per dish in the absence and 5,000 dpm per dish in the presence of an excess amount of unlabeled L-proline. Values are mean ± SE, $n = 4$ for each point

Beginning at day 2 we measured the uptake of L-[^{3}H]proline (15 nM) at an extracellular pH of 6.0 in the absence of sodium, thereby ensuring optimal conditions for pH dependent L-proline transporters (Brandsch 2006). In undifferentiated 3T3-L1 cells the L-[^{3}H]proline uptake rate varied between 0 and 0.3 pmol/10 min per mg of protein (Fig. 1). In differentiating cells, the uptake of L-[^{3}H]proline increased rapidly and reached an uptake rate of about

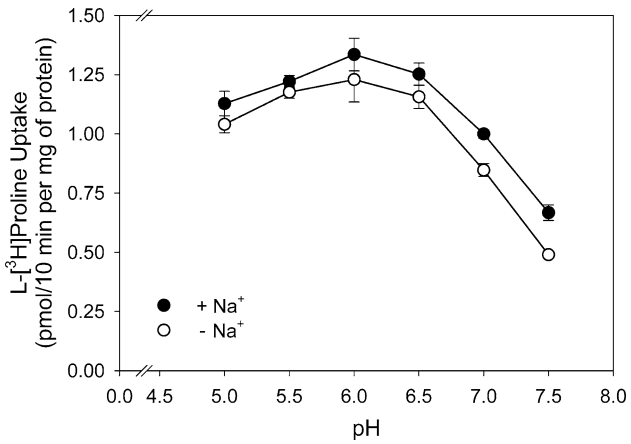

Fig. 3 pH dependency of L-[^{3}H]proline uptake in differentiated 3T3-L1 adipocytes. Uptake of L-[^{3}H]proline (15 nM; 10 min) was measured in the presence (*filled circle*) and absence of sodium (*open circle*) at varying pH values (range 5.0–7.5). Values are mean ± SE, $n = 4$ for each point

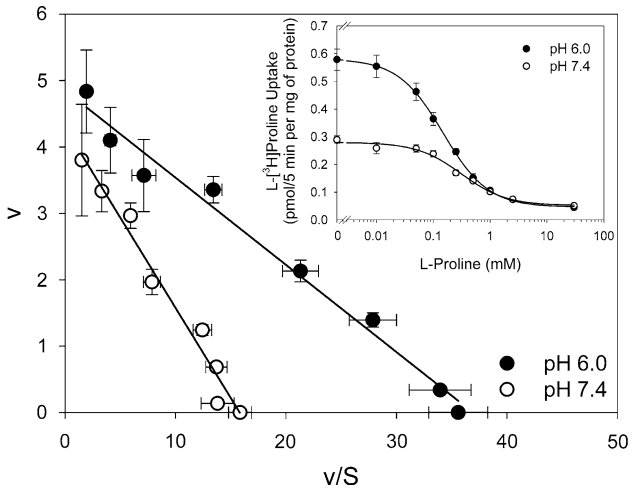

Fig. 4 Effect of pH on the substrate saturation kinetics of specific L-proline uptake in differentiated 3T3-L1 adipocytes. Uptake of L-[^{3}H]proline (15 nM, 5 min, pH 6.0 or pH 7.4) was measured in the absence of sodium at varying concentrations of unlabeled L-proline (0–30 mM). Eadie-Hofstee transformation of the data was performed after subtracting the diffusional/binding component determined by measuring L-[^{3}H]proline uptake in the presence of 30 mM L-proline to obtain the specific carrier-mediated uptake. *v* Uptake rate in nmol/5 min per mg of protein, *S* L-proline concentration in mM, *Inset* Original data of L-[^{3}H]proline uptake inhibited by increasing concentrations of L-proline (10–30 mM). Values are mean ± SE, $n = 6$ for each point

1.4 pmol/10 min per mg of protein. We concluded that the macro- and microscopically evident differentiation of 3T3-L1 cells correlates strongly with their H^+ gradient-stimulated uptake of radiolabeled L-proline.

Next, we examined the time, Na^+ and pH dependence of L-[^{3}H]proline uptake in 3T3-L1 adipocytes (Fig. 2). L-[^{3}H]Proline uptake was linear for at least 5 min; this period was later chosen for determination of kinetic parameters. Replacing 140 mM NaCl with 140 mM choline chloride in the uptake buffer at pH 6.0 or pH 7.4 had no significant effect on L-[^{3}H]proline uptake. At both pH values, the uptake of L-[^{3}H]proline was Na^+-independent. Uptake was also independent of an inwardly directed chloride gradient. At pH 7.4, L-[^{3}H]proline uptake was 0.46 ± 0.02 pmol × 5 min^{-1} mg of $protein^{-1}$ in Na^+-free buffer with Cl^- and 0.45 ± 0.04 pmol 5 min^{-1} mg of $protein^{-1}$ in Na^+- and Cl^- -free buffer. L-[^{3}H]Proline uptake was, however, strongly stimulated by an extracellular pH of 6.0 (Fig. 2). The transport of L-[^{3}H]proline (15 nM) was highly saturated by addition of an excess amount of unlabeled L-proline: 30 mM L-proline inhibited the uptake of L-[^{3}H]proline by more than 90 % (Fig. 2).

To determine the pH optimum of transport, L-[^{3}H]proline uptake in 3T3-L1 adipocytes was measured over an extracellular pH range from 5.0 to 7.5 (Fig. 3). Both in the absence and the presence of a sodium gradient, an uptake maximum at pH 6.0 was observed. Uptake measured at pH 6.0 was 2.5 fold higher compared to uptake at pH 7.5. Interestingly, at all pH values measured, the L-[^{3}H]proline uptake in the presence of a Na^+ gradient was slightly higher than in its absence. The most likely reason for this observation could be a small but measurable contribution of one or more sodium-coupled amino acid transporters that accept L-proline as a substrate (Brandsch 2006). On the other hand, a long incubation of cells in the absence of Na^+ might also lead to an inner acidification because protons entering the cells via amino acid—proton cotransport are not removed by Na^+/H^+ exchangers when no extracellular Na^+ is present (Thwaites et al. 1995; Thwaites and Anderson 2007).

Table 1 Substrate specificity of L-[^{3}H]proline uptake in differentiated 3T3-L1 cells

Compound	pH 6.0		pH 7.4	
	L-[^{3}H]Proline uptake (%)[a]	K_i (mM)	L-[^{3}H]Proline uptake (%)[a]	K_i (mM)
Control	100 ± 2	–	100 ± 1	–
Glycine	27 ± 3*	0.95 ± 0.12	43 ± 1*	2.1 ± 0.2
L-Alanine	13 ± 1*	0.26 ± 0.01	27 ± 1*	0.41 ± 0.02
L-Proline	9 ± 1*	0.16 ± 0.01	23 ± 1*	0.28 ± 0.03
L-Cysteine	84 ± 4	–	–	–
L-Valine	86 ± 4	–	–	–
L-Tryptophan	34 ± 2*	2.0 ± 0.1	55 ± 2*	3.3 ± 0.1
Taurine	94 ± 4	–	90 ± 4	–
GABA	92 ± 6	–	93 ± 7	–

Uptake of L-[^{3}H]proline (15 nM) was measured at pH 6.0 or pH 7.4 for 10 min or 5 min, respectively, in the absence of sodium and in the absence (100 %) or presence of varying concentrations of unlabeled compounds. K_i values were calculated from curves shown in Fig. 5. Values are mean ± SE with $n = 4$–6 for each data point

* Significant from control, $p \leq 0.05$

[a] At a fixed inhibitor concentration of 5 mM

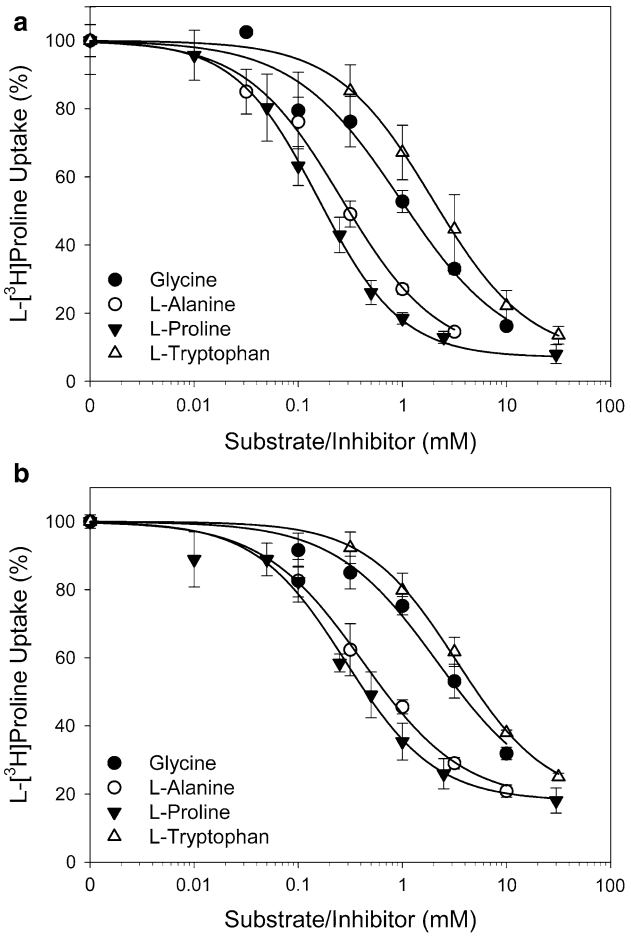

Fig. 5 Inhibition of L-[^{3}H]proline uptake in differentiated 3T3-L1 adipocytes. Uptake of L-[^{3}H]proline (15 nM) was measured at increasing concentrations of unlabeled amino acids at pH 6.0 for 10 min (**a**) or at pH 7.4 for 5 min (**b**). L-[^{3}H]Proline uptake measured in the absence of unlabeled compounds was taken as 100 %. Values are mean ± SE, $n = 4$ for each point

The pH profile obtained in this experiment is very similar to that obtained in studies at PAT2-expressing *X. laevis* oocytes. It differs, however, significantly from the pH dependence of PAT1 and PAT4: Even though at both PAT1 and PAT2 an optimum of around pH 5.5 has been obtained for substrate uptake into oocytes, uptake by PAT1 is almost abolished at pH 7.4 (<10 % compared to pH 5.5) whereas uptake by PAT2 at pH 7.4 still occurs at half maximum (Boll et al. 2002; Kennedy et al. 2005). Hence, substrate transport by PAT1 depends more strictly on an acidic pH_o than substrate transport by PAT2. In contrast to both systems, PAT4 shows a maximal L-proline transport rate at pH 7.4 and is inhibited at acidic pH (Pillai and Meredith 2011).

It is well known that PAT1 and PAT2 differ strongly in their affinity towards substrates. Therefore, we next determined the apparent affinity constant (K_t) and the maximal velocity (V_{max}) of L-proline uptake in 3T3-L1 adipocytes. L-[^{3}H]Proline uptake was measured in the absence of sodium at pH 6.0 and at pH 7.4 for 5 min at increasing concentrations of unlabeled L-proline. At both pH values unlabeled L-proline strongly and dose-dependently inhibited the uptake of L-[^{3}H]proline (Fig. 4 inset). The non-mediated uptake components representing simple diffusion plus unspecific binding of the tracer were determined by measuring the L-[^{3}H]proline uptake in the presence of 30 mM unlabeled L-proline. These non-saturable components (8 % at pH 6.0 and 18 % at pH 7.4) of total L-[^{3}H]proline uptake (Fig. 4 inset) were subtracted from the total L-[^{3}H]proline uptake to determine the specific carrier-mediated uptake rate. The relationship between this rate and the L-proline concentration was found to be hyperbolic at both pH values and was plotted in form of an Eadie-Hofstee graph (Fig. 4). In these plots, straight lines were obtained indicating that only one saturable system is involved in the L-proline uptake. The kinetic parameters derived from these data were as follows: At pH 6.0, the K_t value was 130 ± 10 µM and the V_{max} value was 4.9 ± 0.2 nmol/5 min per mg of protein. At pH 7.4, K_t was increased to 270 ± 20 µM and the V_{max} remained very similar (4.3 ± 0.2 nmol/5 min per mg of protein). In other words, changing the pH from 7.4 to 6.0 affected the apparent affinity constant but not the maximal velocity of transport. Substrate transport is stimulated by acidic pH due to an increased apparent affinity of the transport protein to its substrate and not due to an increased turnover rate of the carrier or other mechanisms contributing to V_{max} changes. This effect of pH is a recognized feature of PAT2 functional activity. For example, Foltz and co-workers (Foltz et al. 2004b) addressed the question in detail by determining the apparent K_t values of glycine and L-alanine at pH values of pH 5.5–8.5 at PAT2-expressing *X. laevis* oocytes. When increasing the pH in the extracellular medium, voltage dependence of the K_t values became pronounced with a severe reduction in affinity.

Compared to the isoform transporter PAT1, PAT2 is classified as the "high affinity, low capacity" transporter (Boll et al. 2002). The kinetic studies leading to this conclusion had been performed with *X. laevis* oocytes expressing the mouse PAT1 or PAT2 cRNA. At pH 6.5, a K_m of 0.12 mM at mPAT2 and a K_m of 2.8 mM at mPAT1 were measured for L-proline (Boll et al. 2002). These values were later confirmed using different expression systems and different species (Bröer et al. 2008; Chen et al. 2003a; Kennedy et al. 2005; Metzner et al. 2004; Thwaites et al. 1993; Thwaites and Anderson 2007). Comparing all these data with our results we conclude that the membrane transport system responsible for proton-coupled L-proline uptake into 3T3-L1 adipocytes is PAT2.

Substrate specificity of pH dependent L-[^{3}H]proline uptake

Another criterion to distinguish PAT2 from PAT1 is the substrate specificity. We studied the uptake of L-proline in 3T3-L1 adipocytes in competition assays, i.e. by measuring the effect of excess amounts of other compounds on the uptake of L-[^{3}H]proline at pH 6.0 or pH 7.4 in the absence of sodium. Table 1 shows the results of the first series of measurements performed at a fixed inhibitor concentration of 5 mM. For the strongest inhibitors, detailed competition studies were then performed to calculate their K_i values (Fig. 5; Table 1). L-Cysteine, L-valine, taurine and γ-aminobutyric acid (GABA) did not significantly inhibit the L-[^{3}H]proline uptake system in 3T3-L1 adipocytes. In contrast, unlabeled L-proline, L-alanine, glycine, and L-tryptophan strongly inhibited L-[^{3}H]proline uptake with K_i values in the range of 0.16 ± 0.01 mM (L-proline) to 2.0 ± 0.1 mM (L-tryptophan) at pH 6.0 and in the range of 0.28 ± 0.03 mM (L-proline) to 3.3 ± 0.1 mM (L-tryptophan) at pH 7.4. The affinity constants correspond very well to published data obtained in heterologous transfection systems: For mPAT2 K_t values for glycine, L-alanine, and L-proline of 0.59, 0.26 and 0.12 mM were reported (pH 6.5, Boll et al. 2002). Similar values were measured for rPAT2 (Chen et al. 2003b; Kennedy et al. 2005). In comparison to mPAT1, where the affinity constants for the prototypical substrates L-proline, L-alanine and glycine range from 2.8 to 7.5 mM (Boll et al. 2002), the K_i values of the same substrates at mPAT2 are 5–30 fold lower, i.e. the affinity to mPAT2 is indeed higher.

The K_i values measured at pH 7.4 are 1.6–2.2 fold higher than their corresponding K_i values measured at pH 6.0 again confirming the effect of pH on ligand affinity (see above).

Taurine and GABA are well known PAT1 substrates inhibiting the transport of L-[^{3}H]proline with K_i values comparable to those of glycine and L-proline (Boll et al. 2002; Brandsch 2006). They were classified as "high to medium affinity substrates" (Metzner et al. 2006). In our study, even at concentrations more than 25 fold higher than the expected K_i (extrapolating from PAT1 and PAT2 data on the concentration necessary to reach 50 % uptake inhibition) they inhibited the L-[^{3}H]proline uptake not significantly (Tab. 1). This phenomenon, *i.e.* the fact that PAT2, in strong contrast to PAT1, does not transport taurine and GABA, is also a recognized feature of PAT2 functional activity (Boll et al. 2002; Kennedy et al. 2005).

PAT2 mRNA expression in differentiating 3T3-L1 cells

On the days the uptake of L-[^{3}H]proline was measured (Fig. 1), we also isolated total mRNA from 3T3-L1 cells and performed RT-PCR with specific primers for mPAT2 and mGAPDH (Fig. 6). In undifferentiated cells cultured in regular medium, i.e. in 3T3-L1 preadipocytes, PAT2 expression could not be detected on days 2, 4, 7 and 9. At days 12, 14 and 16 bands of the expected size were observed. Differentiated 3T3-L1 adipocytes, however, showed expression of PAT2 mRNA from day 7 on. We conclude that the H^+-stimulated, Na^+-independent L-[^{3}H]proline uptake correlates not only with the macro-

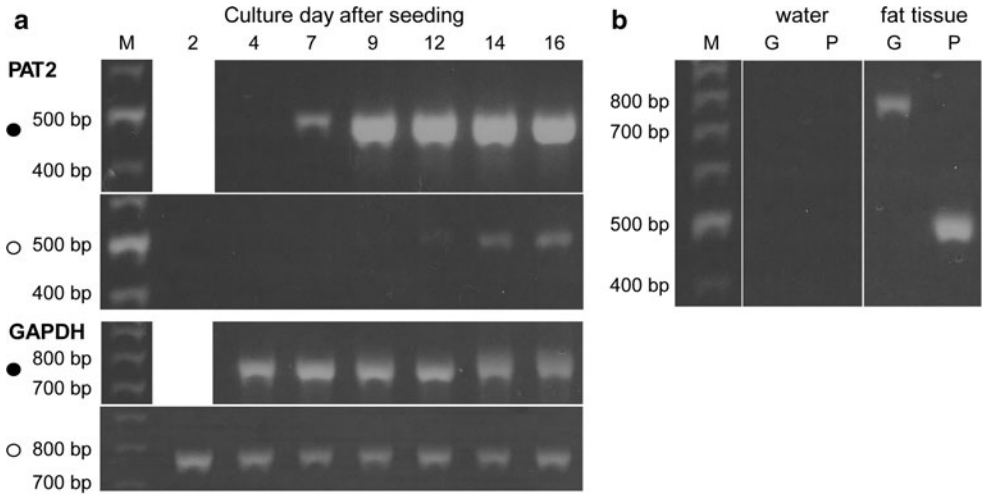

Fig. 6 Influence of growth state on mRNA in 3T3-L1 preadipocytes (*open circle*) and 3T3-L1 cells differentiating to adipocytes (*filled circle*). **a** RT-PCR with total RNA isolated from 3T3-L1 cells at indicated growth states using mPAT2 and mGAPDH specific primers. Specific fragments of GAPDH and PAT2 were reverse-transcribed, amplified and analyzed by agarose gel electrophoresis. The expected sizes of the products were 760 bp for GAPDH and 492 bp for PAT2, respectively. Lane M shows DNA markers with sizes indicated. **b** Positive control reactions (fat tissue) showed bands at the expected sizes and negative control reactions in the absence of template RNA (water) showed no visible band for GAPDH (G) and PAT2 (P)

and microscopically evident differentiation of 3T3-L1 cells but also with the qualitative appearance of PAT2 mRNA in 3T3-L1 adipocytes.

The cell line can be used for PAT2 studies in general, e.g. on regulatory aspects of PAT2 activity, and for studies on the specific function of PAT2 in fat tissue metabolism in particular.

Acknowledgments This work was supported by the Deutsche Forschungsgemeinschaft grant # BR 2430/4-3. The authors thank Valerie Voigt for assistance in PCR measurements. This work will be part of the doctoral thesis of Katja Zebisch.

Conflict of interest The authors declared no conflict of interest.

Ethical standards The experiments comply with the current laws of the country in which they were performed.

References

Bermingham JR Jr, Pennington J (2004) Organization and expression of the SLC36 cluster of amino acid transporter genes. Mamm Genome 15:114–125

Bermingham JR Jr, Shumas S, Whisenhunt T, Sirkowski EE, O'Connell S, Scherer SS, Rosenfeld MG (2002) Identification of genes that are downregulated in the absence of the POU domain transcription factor pou3f1 (Oct-6, Tst-1, SCIP) in sciatic nerve. J Neurosci 22:10217–10231

Boll M, Foltz M, Rubio-Aliaga I, Kottra G, Daniel H (2002) Functional characterization of two novel mammalian electrogenic proton-dependent amino acid cotransporters. J Biol Chem 277:22966–22973

Boll M, Foltz M, Anderson CMH, Oechsler C, Kottra G, Thwaites DT, Daniel H (2003a) Substrate recognition by the mammalian proton-dependent amino acid transporter PAT1. Mol Membr Biol 20:261–269

Boll M, Foltz M, Rubio-Aliaga I, Daniel H (2003b) A cluster of proton/amino acid transporter genes in the human and mouse genomes. Genomics 82:47–56

Boll M, Daniel H, Gasnier B (2004) The SLC36 family: proton-coupled transporters for the absorption of selected amino acids from extracellular and intracellular proteolysis. Pflügers Arch 447:776–779

Brandsch M (2006) Transport of L-proline, L-proline-containing peptides and related drugs at mammalian epithelial cell membranes. Amino Acids 31:119–136

Bröer S, Bailey CG, Kowalczuk S, Ng C, Vanslambrouck JM, Rodgers H, Auray-Blais C, Cavanaugh JA, Bröer A, Rasko JEJ (2008) Iminoglycinuria and hyperglycinuria are discrete human phenotypes resulting from complex mutations in proline and glycine transporters. J Clin Invest 118:3881–3892

Chen Z, Fei YJ, Anderson CMH, Wake KA, Miyauchi S, Huang W, Thwaites DT, Ganapathy V (2003a) Structure, function and immunolocalization of a proton-coupled amino acid transporter (hPAT1) in the human intestinal cell line Caco-2. J Physiol 546:349–361

Chen Z, Kennedy DJ, Wake KA, Zhuang L, Ganapathy V, Thwaites DT (2003b) Structure, tissue expression pattern, and function of the amino acid transporter rat PAT2. Biochem Biophys Res Commun 304:747–754

Edwards N, Anderson CMH, Gatfield KM, Jevons MP, Ganapathy V, Thwaites DT (2011) Amino acid derivatives are substrates or non-transported inhibitors of the amino acid transporter PAT2 (slc36a2). Biochim Biophys Acta 1808:260–270

Foltz M, Boll M, Raschka L, Kottra G, Daniel H (2004a) A novel bifunctionality: PAT1 and PAT2 mediate electrogenic proton/amino acid and electroneutral proton/fatty acid symport. FASEB J 18:1758–1760

Foltz M, Oechsler C, Boll M, Kottra G, Daniel H (2004b) Substrate specificity and transport mode of the proton-dependent amino acid transporter mPAT2. Eur J Biochem 271:3340–3347

Green H, Kehinde O (1974) Sublines of mouse 3T3 cells that accumulate lipid. Cell 1:113–116

Hediger MA (2004) The ABC of solute transporters. Pflügers Arch 447:5

Kennedy DJ, Gatfield KM, Winpenny JP, Ganapathy V, Thwaites DT (2005) Substrate specificity and functional characterisation of the H^+/amino acid transporter rat PAT2 (Slc36a2). Br J Pharmacol 144:28–41

Klein C, Scoggin KE, Ealy AD, Troedsson MHT (2010) Transcriptional profiling of equine endometrium during the time of maternal recognition of pregnancy. Biol Reprod 83:102–113

Larsen M, Holm R, Jensen KG, Brodin B, Nielsen CU (2009) Intestinal gaboxadol absorption via PAT1 (SLC36A1): modified absorption in vivo following co-administration of L-tryptophan. Br J Pharmacol 157:1380–1389

Metzner L, Kalbitz J, Brandsch M (2004) Transport of pharmacologically active proline derivatives by the human proton-coupled amino acid transporter hPAT1. J Pharmacol Exp Ther 309:28–35

Metzner L, Kottra G, Neubert K, Daniel H, Brandsch M (2005) Serotonin, L-tryptophan, and tryptamine are effective inhibitors of the amino acid transport system PAT1. FASEB J 19:1468–1473

Metzner L, Neubert K, Brandsch M (2006) Substrate specificity of the amino acid transporter PAT1. Amino Acids 31:111–117

Pillai SM, Meredith D (2011) SLC36A4 (hPAT4) is a high affinity amino acid transporter when expressed in Xenopus laevis oocytes. J Biol Chem 286:2455–2460

Ranaldi G, Islam K, Sambuy Y (1994) D-cycloserine uses an active transport mechanism in the human intestinal cell line Caco 2. Antimicrob Agents Chemother 38:1239–1245

Rubio-Aliaga I, Boll M, Vogt-Weisenhorn DM, Foltz M, Kottra G, Daniel H (2004) The proton/amino acid cotransporter PAT2 is expressed in neurons with a different subcellular localization than its paralog PAT1. J Biol Chem 279:2754–2760

Sagné C, Agulhon C, Ravassard P, Darmon M, Hamon M, El Mestikawy S, Gasnier B, Giros B (2001) Identification and characterization of a lysosomal transporter for small neutral amino acids. Proc Natl Acad Sci USA 98:7206–7211

Sundberg BE, Wååg E, Jacobsson JA, Stephansson O, Rumaks J, Svirskis S, Alsiö J, Roman E, Ebendal T, Klusa V, Fredriksson R (2008) The evolutionary history and tissue mapping of amino acid transporters belonging to solute carrier families SLC32, SLC36, and SLC38. J Mol Neurosci 35:179–193

Thwaites DT, Anderson CMH (2007) Deciphering the mechanisms of intestinal imino (and amino) acid transport: the redemption of SLC36A1. Biochim Biophys Acta 1768:179–197

Thwaites DT, Anderson CM (2011) The SLC36 family of proton-coupled amino acid transporters and their potential role in drug transport. Br J Pharmacol 164:1802–1816

Thwaites DT, McEwan GTA, Cook MJ, Hirst BH, Simmons NL (1993) H^+-coupled (Na^+-independent) proline transport in human intestinal (Caco-2) epithelial cell monolayers. FEBS Lett 333:78–82

Thwaites DT, McEwan GTA, Simmons NL (1995) The role of the proton electrochemical gradient in the transepithelial absorption of amino acids by human intestinal Caco-2 cell monolayers. J Membr Biol 145:245–256

Vanslambrouck JM, Bröer A, Thavyogarajah T, Holst J, Bailey CG, Bröer S, Rasko JEJ (2010) Renal imino acid and glycine transport system ontogeny and involvement in developmental iminoglycinuria. Biochem J 428:397–407

Zebisch K, Voigt V, Wabitsch M, Brandsch M (2012) Protocol for effective differentiation of 3T3-L1 cells to adipocytes. Anal Biochem 425:88–90